

See discussions, stats, and author profiles for this publication at: <https://www.researchgate.net/publication/313770331>

PREDICTION OF AVERAGE VOID FRACTION AND PDF OF VOID FRACTION IN VERTICAL 90° BEND FOR AIR–SILICONE OIL FLOW USING MULTILAYER PERCEPTRON (MLP) CODES

Article · January 2017

CITATIONS

4

READS

1,916

1 author:



Paul Ayegba

Institut de Mécanique des Fluides de Toulouse

10 PUBLICATIONS 16 CITATIONS

SEE PROFILE

Some of the authors of this publication are also working on these related projects:



DRAG REDUCTION IN CURVES AND BENDS FOR OIL-WATER FLOW [View project](#)



Multiphase flow in bends [View project](#)



PREDICTION OF AVERAGE VOID FRACTION AND PDF OF VOID FRACTION IN VERTICAL 90° BEND FOR AIR–SILICONE OIL FLOW USING MULTILAYER PERCEPTRON (MLP) CODES

Paul Onubi Ayegba^{a*}, Mukhtar Abdulkadir^b

^a Chemical Engineering Department, Faculty of Engineering, Ahmadu Bello University, P.M.B. 1094 Samaru, Zaria, Nigeria. National Environmental Standards and Regulations Enforcement Agency, North-west zonal Headquarters, Kano, Nigeria.

^b Mukhtar Abdulkadir, Manufacturing Engineering Research Division, Faculty of Engineering, University of Nottingham University Park, Nottingham, NG7 2RD, United Kingdom. Chemical Engineering Department, Federal University of Technology, Minna, Nigeria. Petroleum Engineering Department, African University of Science and Technology (AUST), Abuja, Nigeria, City

ABSTRACT

Multilayer Perceptron (MLP) models have been developed to predict two-phase average void fraction and probability density function (PDF) of void fraction in 90° bends. The Artificial Neural Network (ANN) methodology was reported using MLP trained with 2 algorithms. Logarithmic sigmoid transfer function was used in a single hidden layer for both algorithms (Gradient descent (GDMV) and Levenberg-Marquardt (LM) algorithms). Both MLP models were optimised by varying the number of neurons in the hidden layer while monitoring the Mean Square Error (MSE). The performance of the models was evaluated using the Average Absolute Relative Error (AARE) and Cross Correlation Coefficient (R). Both MLP models developed for the prediction of average void fraction before the bend performed excellently well. However, the MLP model trained with LM algorithm having 3 neurons in the hidden layer gave better performance. Similarly, the MLP model trained with LM algorithm, having 11 neurons in the hidden layer for the prediction of PDF of void fraction before the bend gave excellent prediction. Model performance for the MLP models after the bend gave poor generalisation property. However, the MLP model based on GDMV algorithm gave better prediction for predicting average void fraction and PDF of void fraction after the bend. It was concluded that MLP models may with some confidence be used to predict the average void fraction and the PDFs of void fraction observed before a vertical 90° bend.

KEYWORDS

90° bend, air–silicone oil; void fraction; MLP; ANN; LM algorithm; GDMV algorithm; Modelling

ARTICLE INFO

Received 18 July 2016
Accepted 25 Dec 2016
Available online 5 Jan 2017

* Corresponding author:

E-mail: paulsnow4christ@gmail.com, Tel.: +2348036837921

1. Introduction

Two phase gas-liquid flows are both common and important in oil and gas production and flow lines of different configurations (Abdulkadir et al. 2011). Two-phase flows are often conveyed through pipes of various configurations as well as pipe fittings such as bends (Tarun & Sudip 2007). According to Abdulkadir (2011) the presence of bends introduces secondary flows, redistribution of multiphase fractions, flow excursions, deviation in flow paths etc. The orientation of the connecting pipe make a difference in the flow patterns for reasons which include sharp deviation in flow path around bends and also because of the role played by gravity and density difference between the two fluids. Two important characteristics of two-phase flows around bends are highly fluctuating voids immediately after bends and changes in flow pattern. It is therefore imperative to develop a means for predicting flow characteristics. A method that has been successfully used for determining flow pattern is the probability density function (PDF) of void fraction. A number of modelling techniques have been employed in the past for void fraction and flow pattern prediction. The models are either empirical, mechanistic or numerical. However, the application of Multilayer Perceptron Modelling (MLP), for the prediction of flow characteristics around bends has received little attention in the peer review literature. Most of the investigations have been restricted to experimental investigation: (Abdulkadir et al. 2011; Carver 1984; Carver & Salcudean 1986; Ellul & Issa 1987; Gardner & Neller 1969; Legius et al. 1995; Saidj et al. 2014), address the issue of gas-liquid systems but most of the reported experiments are not extended to the application of MLP to predict such flows in bends.

MLP modelling is a type of numerical modelling. Numerical modelling technique is a useful tool in visualising the dynamic behaviour of real systems. It has a unique advantage in that there is no limit to the complexity of problem it can solve (Soetaert & Herman 2009). MLP models are similar to ANN and are based on the concept of interconnected systems of simple-processing units (Carlos 2011).

1.1. The Back-propagation Algorithm

In back-propagation algorithms the processing elements are arranged in layers, signals are sent forward while errors are propagated backwards. The layers consist of input, hidden and outputs layers. The number of processing elements in the input layer is defined by the number of independent input variables, while that of the hidden layer is determined by method of optimisation. There may be one or more intermediate hidden layers as illustrated in Figure 1.

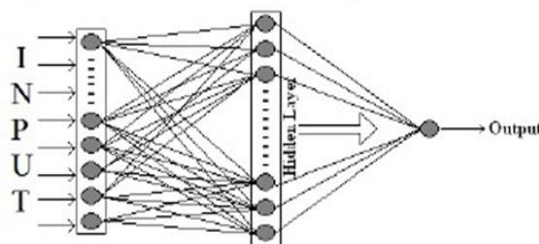


Figure 1. Schematic diagram of the ANN (Bar & Das 2012)

Generally MLP modelling similar to ANN use either supervised or unsupervised learning during the process of model training. The method used in back-propagation algorithm is supervised learning, which means that

the user provides the algorithm with examples of the inputs and outputs for the network to compute, and then the error (difference between actual and expected results) is calculated. The concept of the back-propagation algorithm is to reduce this error, until the ANN learns the training data. The training usually begins with random weights (or user specified weights), and the goal is to adjust them so that the error will be minimal (Carlos 2011).

1.2. Two-phase flow in 90° bends

A number of experimental and modelling studies have been carried out in the past for two phase gas-liquid flows in bends. Majority of these works were for air-water systems and very few used advanced instrumentation for their investigation. A Visual and experimental study for two-phase flow through a transparent pipe 76-mm diameter was carried out by Gardner and Neller (1969). Their flow facility consisted of a vertical 90° bends of 305 and 610 mm radii of curvature. The investigation for limited to bubble and slug flow regimes for air-water flow. The goal was to interrogate the competitive effects of centrifugal and gravity forces on the ensuing flow distribution in bends. A 2D modelling study was carried out by Carver, (1984) for flow around a vertical 90° bends. Model predictions from their work were compared results of experimental investigation of (Gardner & Neller 1969). The results showed poor correlation between model predictions and experimental measurements. An extension of the 2D model to a 3D model was carried out by Carver and Salcudean (1986) who obtained better model predictions for experimental measurements. Ellul and Issa (1987) developed an improved 3-D numerical simulation, in which a substantially different solution algorithm, with an additional momentum term, was adopted. They applied the models to both air-water and gas-oil mixtures. The predicted simulation flow data gave better agreement with the experimental data compared to those obtained by the 2-D model in (Carver 1984). There was, however, a shortage of experimental data at the time for validation of their gas-oil simulation. An experimental and numerical modelling study was carried out by Legius, Narumo and Van-den-Akker (1995) for air-water flow in a bend of 630 mm radius of curvature. The flow configuration was horizontal to vertical though the bend and the pipe were made of transparent acrylic material of internal diameter 100-mm. Visual observations of the flow regime was done using a 200 Hz digital camera and an auto-regressive modelling method. They observed two flow regimes (Slug and churn flow) in the riser and three flow regimes (stratified, slug and enhanced slug) in the horizontal pipe section. The time dependent behaviour of two-phase flow was modelled by an in-house code named Solution Package for Hyperbolic Functions (SOPHY-2). In most of the tested data an excellent agreement was found between the experimental and modelling results. Abdulkadir et al. (2011) used electrical capacitance tomography (ECT), high speed video and wire mesh sensor (WMS) to interrogate the effects of 90° bends on two-phase air-silicone oil flows. The downstream pipe was kept horizontally while the upstream pipe was vertical. The characteristic PDF of void fraction for various flow rates were used to identify the flow regime upstream and downstream of the bend. They observed bubble, stratified, slug and semi-annular flows downstream of the vertical 90° bend while the flow patterns exhibited upstream of the bend was the same as for the horizontal 90° bend. Saidj et al. (2014) conducted an experimental study of the behaviour of two-phase air-water flow from the vertical to the horizontal through a 90° bend using conductance probes technique. Void fraction measurement was done using the conductance probes (3 upstream and 6 downstream of the bend). The characteristic PDF of void fraction, power spectral density (PSD) of the time series of cross sectional average void fraction and visual observations were used to characterize the flow behaviour. For the horizontal pipe, plug, slug and stratified wavy flow patterns were seen while slug and churn flows in the vertical pipe.

1.3. Application of Artificial Neural Network (ANN) methodology to gas-liquid flows

Hernandez et al. (2006) used ANN to process signals measured using a conductivity probe with the aim of classifying them into various flow patterns. They used visual map identification to validate the results of ANN model predictions. The ANN predictions were in good agreement with results of visual identification. A comparative model study was carried out by Nasseh et al. (2007) for the prediction of pressure loss in

five venture scrubbers. They compared the results of ANN prediction with a number of other models and concluded that predictions of the ANN models were better within the range of data tested. Zhigiang and Z. Hongjian (2008) used adopted inputs, all representing the characteristics of PSD, in training a three-layered feed forward ANN for the prediction of flow pattern. The model predictions gave good agreement to the observed flow patterns. A comparative study of CFD and ANN was carried out by Asghar, Masoud and Abdulaziz (2009). They used both CFD and ANN for the prediction of pressure drop in two phase gas-liquid flows in 2-cm diameter, 6-m long pipe. The inputs to their ANN model were gas velocity, liquid velocity and tube inclination. Predictions from both models indicated that the CFD model performed better. Ayoub and Demiral (2011) used ANN technique in predicting the pressure drop observed in three phase flow conditions. The resilient back-propagation algorithm was used to formulate the ANN model. This method gave correlation coefficients up to 98.82 %. Santoso and Thomas (2012) employed ANNs in characterizing observed flow pattern. The method was based upon an analysis of the PSD determined from the differential pressures measured within a horizontal pipe conveying. Over the range of data tested, model predictions were in good agreement with experimental data. Three different ANN algorithms were used by (Bar & Das 2012) to predict the observed void fractions and pressure drops for a two-phase flow in horizontal pipe. The model based on Levenberg Marquardt ANN algorithm with five processing elements gave the best prediction of void fraction and that based on back-propagation ANN algorithm with fifteen processing elements performed best for the prediction of pressure drop. Later, Nirjhar and Sudip (2013) applied a similar methodology for the prediction of flow regime of air–water flow in circular micro channels with reasonable success. Bar, Das and Biswas (2013) further applied ANNs in predicting frictional pressure drop in U-bends. Model predictions gave fairly accurate results of the frictional pressure drop across U-bends. Probabilistic Neural Network (PNN) was used by Karimi et al. (2014) for flow pattern identification. The range of gas and liquid superficial velocity tested were 0.0026-6.05 m/s and 0.03-2.5 m/s respectively. Within this range they observed five different flow patterns. The accuracy of the PNN when it was used to predict flow patterns was as high as 95.6%. An attempt to predict flow patterns for two phase flow was done by Mustafa, Moustafa and Abdulsalam (2015). They used three pairs of inputs (gas velocity and liquid velocity, total pressure and liquid hold-up, Reynolds number for liquid and gas). The study was conducted in a horizontal pipe for four different flow regimes (Annular, Dispersed bubble, intermittent and stratified). Their model predicted over 80% of the flow patterns correctly and performed particularly well within the dispersed bubble region for all input pairs. In general the input pair of the natural logarithm of gas and liquid velocity gave better prediction.

The above literature survey show that limited work has been done in the use of MLP, ANN methodology for the prediction of average void fraction and PDF of void fraction in 90o bends for two-phase flows through large diameter pipes. Most of the research has been centred on empirical and visualization techniques. Most of the works that use ANN methodology are those for pressure drop and flow pattern prediction.

2. Experimental Methodology

A summary of the experimental facility is provided in (Abdulkadir et al. 2013; Abdulkadir et al. 2011). The experimental test section of the facility is made of a 67-mm internal diameter a transparent acrylic pipe of 6 m length.

A vertical 90o bend with a radius of curvature 154 mm was made of the straight pipe as shown in Figure 2. Downstream of the bend there is another straight pipe from which the air – silicone oil mixture enters a flexible pipe that takes it to the phase separator. The behaviour of the air – silicone oil mixture was examined using WMS. This technology,

described by (Thiele et al. 2008), can image the dielectric components in the pipe flow phases by measuring rapidly and continually the capacitances of the passing flow across several crossing points in the mesh.

The WMS was first placed at about 4.92 m (73 diameters) away from the mixing section. WMS was afterwards moved to a distance of about 0.21 m (3 diameters) after the bend. The experiments were all performed at an ambient laboratory temperature of 20 ± 0.5 and a pressure of 1 bar.

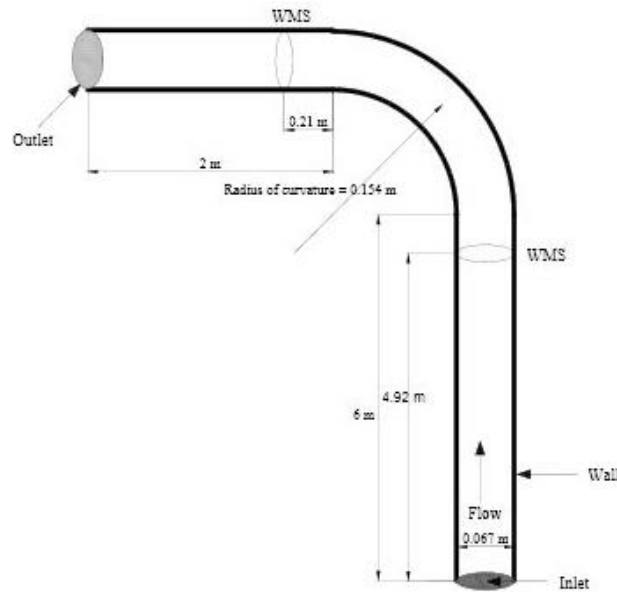


Figure 2. 3-D geometry of the computational domain showing the measurement locations and instrumentation

Table 1. Properties of the fluid at 1 bar and at the operating temperature of $20 \pm 0.5^\circ\text{C}$

Fluid	Density (kgm^{-3})	Viscosity ($\text{kgm}^{-1}\text{s}^{-1}$)	Surface tension (Nm^{-1})	Thermal conductivity ($\text{Wm}^{-1}\text{K}^{-1}$)
Air	1.18	0.000018	0.02	0.1
Silicone oil	900	0.00525		

Table 2. Inlet flow rates (model inputs)

	Before Bend			After Bend		
U_{SL}	0.05	0.14	0.38	0.05	0.14	0.38
	0.047	0.047	0.047	0.047	0.047	0.061
	0.061	0.061	0.061	0.061	0.061	0.288
	0.288	0.288	0.288	0.288	0.288	0.344
	0.344	0.344	0.344	0.344	0.344	0.404
U_{SG}	0.404	0.404	0.404	0.404	0.404	0.544
	0.544	0.544	0.544	0.544	0.544	0.709
	0.709	0.709	0.709	0.709	0.709	1.891
	0.945	0.945	0.945	0.945	1.891	2.363
	1.418	1.418	1.418	1.418	2.363	2.836
	1.891	1.891	1.891	1.891	2.836	4.73
	2.363	2.363	2.363	2.363	4.73	
	2.836	2.836	2.836	2.836		

The experimental data collected using WMS was time series void fractions for 38 experimental data sets before the bend and 33 experimental data sets for after the bend scenario.

The input parameters to the ANNs are the gas and liquid superficial velocities. Parameters like liquid and gas densities, liquid and gas viscosities, surface tension and thermal conductivity of liquid were not used in the formulation of the ANN model formulation as they were assumed to remain constant. The input parameters are summarised in Table 2. The output parameters are time averaged cross sectional area void fraction and PDF of void fraction.

3. Multilayer Perceptron Modelling (MLP)

Two MLP codes that mimic Artificial Neural Networks (ANN) models were developed in this paper for the prediction of average void fraction and PDF of void fraction of gas-liquid flow in 90o bends. The MLP codes were developed in MATLAB and are based on the back-propagation algorithms (Gradient Descent (DC) and Levenberg-Marquardt (LM)). The model topography is such that each model consists of three layers (input, hidden and output layers). The transfer function used in the hidden layer is the logsigmoid (logsig) function given by Equation (1).

$$\text{logsig}(wx) = \frac{1}{(1+\exp(-wx))} \quad (1)$$

Where w is the weight function and x represents the vector input (gas and liquid superficial velocities in this case).

3.1. Gradient descent algorithm (GDMV)

This is regarded as the simplest of all the back-propagation algorithms. It is a first order algorithm and employs the generalised delta rule and weights are updated using the formula;

$$\Delta w_{ij}(t) = -\eta \cdot \frac{\partial E}{\partial w_{ij}} \quad (2)$$

$$w_{ij}(t + 1) = w_{ij}(t) + \Delta w_{ij}(t) \quad (3)$$

Where η is the step size.

The gradient descent algorithm has a tendency to be slow in terms of convergence (Hao & Wilamowski 2010). This slowness is often addressed by using a variable step size and a ‘momentum term’. When the momentum term is added to Equation (3) Equation (4) is obtained;

$$w_{ij}(t + 1) = w_{ij}(t) + \Delta w_{ij}(t) + \alpha \Delta w_{ij}(t - 1) \quad (4)$$

E , is the error function, w_{ij} is the weight matrix and Δw_{ij} is the weight update for each iteration. The error function E , used for this work is Sum of Squares of error. Error here refers to the difference between the model output and experimental output.

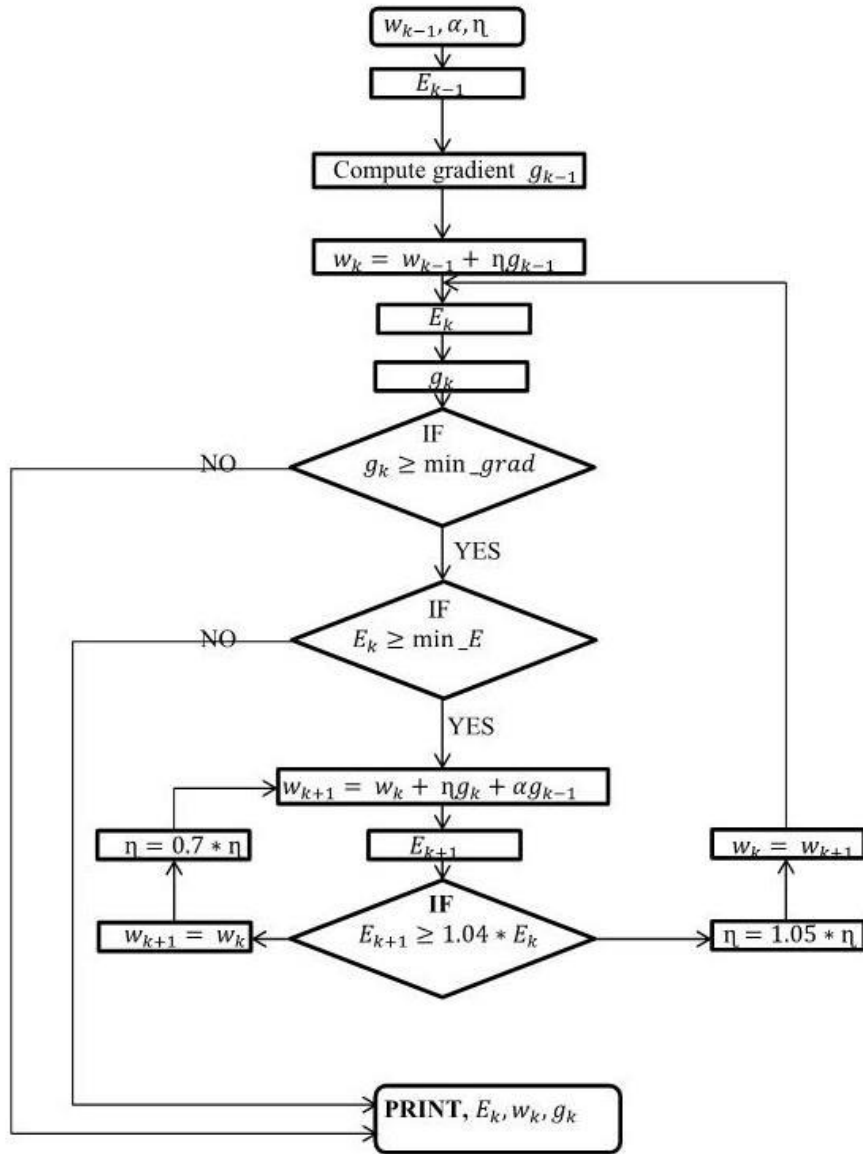


Figure 3. Gradient descent algorithm (with variable step size and momentum term) flowchart

The target is to minimise the partial derivative in Equation (2) (i.e. the gradient of the error function) to zero. First order algorithms has the inherent disadvantage of being slow, but also has a unique advantage, in that the gradient term can be minimised to zero with sufficient amount of iterations.

Figure 3 and 4 depict flow charts of the gradient descent and Levenberg-Marquardt algorithms respectively that were developed here.

3.2. Levenberg-Marquardt algorithm (LM)

The Levenberg-Marquardt algorithm combines of Gauss-Newton algorithm (a second order algorithm) and gradient descent algorithm (a first order learning algorithm). Generally, second order algorithm converges much faster than the first order algorithms.

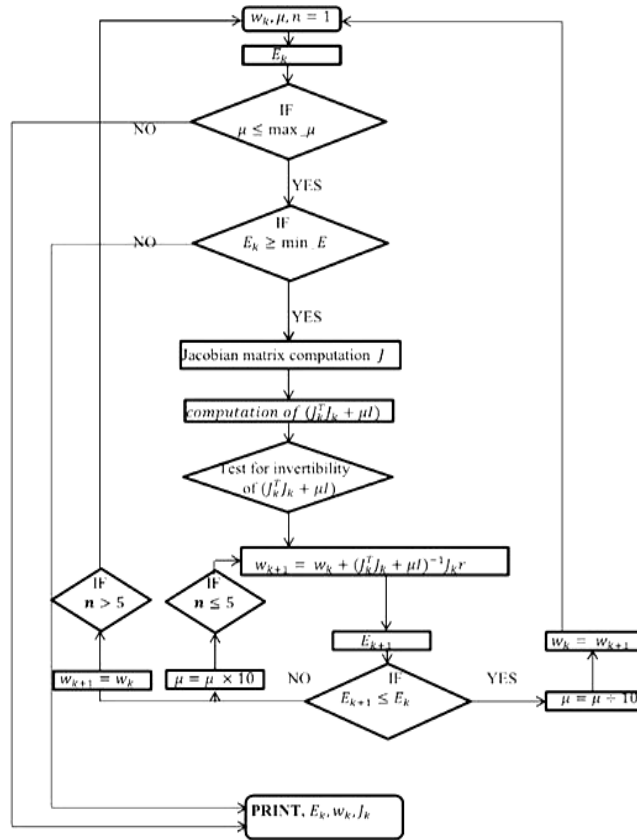


Figure 4. Levenberg-Marquardt algorithm flowchart

The update rule of Levenberg–Marquardt algorithm can be presented as

$$w_{k+1} = w_k - (J_k^T J_k + \mu I)^{-1} \cdot J_k e \quad (5)$$

J_k is the Jacobian matrix given by;

$$J_k = \begin{bmatrix} \frac{\partial e_{1,1}}{\partial w_1} & \frac{\partial e_{1,1}}{\partial w_2} & \dots & \frac{\partial e_{1,1}}{\partial w_N} \\ \frac{\partial e_{1,2}}{\partial w_1} & \frac{\partial e_{1,2}}{\partial w_2} & \dots & \frac{\partial e_{1,2}}{\partial w_N} \\ \dots & \dots & \dots & \dots \\ \frac{\partial e_{1,M}}{\partial w_1} & \frac{\partial e_{1,M}}{\partial w_2} & \dots & \frac{\partial e_{1,M}}{\partial w_N} \\ \frac{\partial e_{P,1}}{\partial w_1} & \frac{\partial e_{P,1}}{\partial w_2} & \dots & \frac{\partial e_{P,1}}{\partial w_N} \\ \frac{\partial e_{P,2}}{\partial w_1} & \frac{\partial e_{P,2}}{\partial w_2} & \dots & \frac{\partial e_{P,2}}{\partial w_N} \\ \dots & \dots & \dots & \dots \\ \frac{\partial e_{P,M}}{\partial w_1} & \frac{\partial e_{P,M}}{\partial w_2} & \dots & \frac{\partial e_{P,M}}{\partial w_N} \end{bmatrix} \text{ Where } e \text{ is given by } e = \begin{bmatrix} e_{1,1} \\ e_{1,2} \\ \dots \\ e_{1,M} \\ \dots \\ e_{P,1} \\ e_{P,2} \\ \dots \\ e_{P,M} \end{bmatrix}$$

Where, μ is always positive, called combination coefficient and \mathbf{I} is the identity matrix.

As the combination of the steepest descent algorithm and the Gauss–Newton algorithm, the Levenberg–Marquardt algorithm switches between the two algorithms during the training process.

3.3. MLP Model Optimization

The optimisation process involves determining the network topology and weights that gives best model performance when tested using certain performance equations. It is important to determine the optimum number of neurons in the hidden layer. This optimum number depends on the number of input and output units, the number of training cases, the amount of noise in the targets, the complexity of the error function, the network architecture, and the training algorithm. In most cases according to Ayoub and Demiral (2011), there is no straight forward method of determining the optimal number of hidden units without training using different numbers of hidden units and estimating the generalization error of each.

In the present work, a single hidden layer with multiple neurons units is used as previous study by Bar and Das (2012) showed that a single hidden layer with sufficient number of neurons performed satisfactorily well. The details of the concept of hidden layer can be found elsewhere, example in (Mark et al. 2012). In the hidden layer the numbers of processing elements are optimized by varying the number from 1 to 25. The basic approach used in constructing the successful model was trial and error. The generalization error (cross validation error) of each inspected network design was visualized and monitored carefully through plotting the governing statistical parameters such as correlation coefficient, root mean squared errors, and average absolute relative error of each inspected topology.

It is worthy of note that various network topology could be employed for MLP model development. However, the back-propagation network with feed-forward algorithm was chosen here as this has performed satisfactorily well in previous works such as (Bansal et al. 1993; Barnard & Wessels 1992; Ayoub & Demiral 2011; Bar & Das 2012; Zhigiang & Z. Hongjian 2008) among others.

3.4. Objective Function and Performance of ANN

The objective function provides the basis for performance evaluation and network algorithm selection. A suitable objective function which provides a good basis for numerical computation and attainment of set goals must be chosen. In this work, sum of squares of error is used as the objective function and it is given by equation (6).

$$E = \frac{1}{2} \sum_{i=1}^N (O_i - t_i)^2 \quad (6)$$

The performance of the network is checked using the following parameters: Mean Squared Error (MSE),

$$MSE = \frac{1}{N} \sum_{i=1}^N (x_i - y_i)^2 \quad (7)$$

Average Absolute Relative Error (AARE)

$$AARE = \frac{1}{N} \sum_{i=1}^N \left| \frac{(y_i - x_i)}{x_i} \right| \quad (8)$$

The AARE eliminates the possibility of obtaining negative values of relative error. The aim is to obtain values of AARE close to zero.

Cross-correlation coefficient (R)

$$R = \frac{\frac{1}{N} \sum_{i=1}^N (x_i - \bar{x})(y_i - \bar{y})}{\sqrt{\sum_{i=1}^N (x_i - \bar{x})^2 \sum_{i=1}^N (y_i - \bar{y})^2}} \quad (9)$$

A value of R unity (1) means there is a perfect correlation between experimental and predicted results, while a value of R close to zero would indicate that there is little or no correlation between experimental and predicted data (Bar & Das 2012). Thus models capable of predicting experimental data such that the value of R is close to one would be considered as good models.

3.5. Developed MLP Algorithms Codes (program development)

Data collection and partitioning, filtering and screening procedure, data randomization, pre-processing, and post-processing were done before running the models. A total number of 38 data sets before the bend and 33 data sets after the bend were utilized for the purpose of this study for modelling ends. Input data are.

The partitioning ratio of 4:1:1 is known to yield better training and testing results (but depends on the number of data set used for training). Other common partitioning ratios are 2:1:1 and 3:1:1 (Bar & Das 2012). For this work, a partitioning ratio of 3:1:1 was adopted. The training set is used to develop and adjust the weights in a network. The validation set is used to ensure the generalization of the developed model during the training phase, and the test set is used to examine the final performance of the model. The primary concerns are to ensure two things: (a) the training set contains enough data, and suitable data distributed evenly to cover the entire range of data, and (b) there is no unnecessary similarity between the data in different sets. The number of iterations for each model was initially put at 100,000 iterations but if performance does not improve much after 10,000 iterations then training is stopped.

The MLP models developed for the prediction of average void fraction before the bend based on gradient descent algorithm and PDF of void fraction after the bend based on Levenberg-Marquardt algorithm are given in the appendix.

4. Results

In this section results model optimization and performance of the developed MLP models are presented.

4.1. Result of MLP model optimization

Figure 4 is a plot of minimum cross-validation MSE against number of processing elements in the hidden layer of a selected MLP. The optimum network configuration is chosen as that which gives the least value of cross-validation MSE, which is the network configuration with the best generalisation capability.

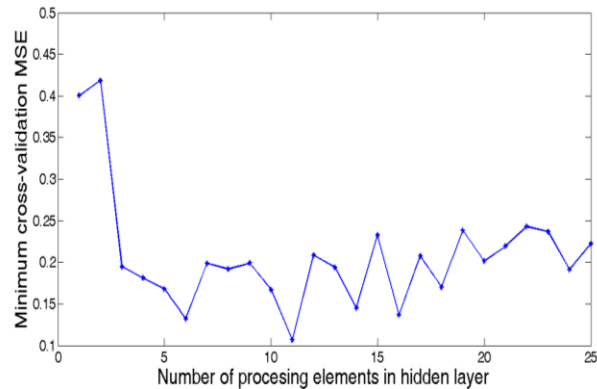


Fig. 5. Minimum cross-validation MSE versus number of processing elements in hidden layer for PDF of void fraction using Levenberg-Marquardt algorithm (before bend).

Table 3 gives the optimum number of neurons in the hidden layer for each MLP model developed. All further analysis will be based on these optimal configurations.

Table 3: Optimum number of neurons

Algorithm	Optimum number of processing elements	
	Average void fraction	PDF of void fraction
GDMV (before bend)	2	4
LM (before bend)	3	11
GDMV (after bend)	16	4
LM (after bend)	2	4

4.2. Performance of the Optimum Network Configurations for Various MLP Codes

Table 4 gives performance of the optimum network configurations for various MLP codes for training, validation and testing.

Table 4: Performance of the optimum network configurations for various MLP codes developed

Algorithm	Performance	Training		Validation		Testing	
		Average void fraction	PDF of void fraction	Average void fraction	PDF of void fraction	Average void fraction	PDF of void fraction
GDMV (before bend)	MSE	9.2514×10^{-4}	0.0284	7.4305×10^{-4}	0.0957	7.8331×10^{-4}	0.0270
	AARE	0.0265	0.7428	0.0939	3529.5	0.0388	8.7071
	R	0.9980	0.9390	0.9991	0.5317	0.9988	0.9255
LM (before bend)	MSE	4.1445×10^{-4}	0.0089	0.0024	0.1065	0.0026	0.0279
	AARE	0.0157	0.6537	0.1590	1.3139	0.0274	0.7866
	R	0.9991	0.9743	0.9977	0.5486	0.9958	0.9342
GDMV (after bend)	MSE	0.0074	0.0686	0.1276	0.2646	0.0267	0.1801
	AARE	0.0567	0.9702	0.3362	32.9285	0.1961	1.5740
	R	0.9855	0.7532	0.1219	0.0808	0.9156	0.4507
LM (after bend)	MSE	0.1709	0.1605	0.1101	0.2731	0.1820	0.3227
	AARE	0.3062	1.0291	0.2622	1.0789	0.7013	2.7625
	R	0.5893	0.5841	0.7863	0.3482	0.9330	0.3458

The performance results for the test set is of greater significance here as it gives an indication of the model's ability to predict the parameters of interest, which is the network's generalisation property. The Average Absolute Relative Error is used in selecting the best model, among the ones developed. Small values of AARE and values of correlation coefficient (R) close to unity (1) indicate good model performance (Bar & Das 2012). The model chosen, from the models tested, for the prediction of average void fraction or PDF of void fraction before or after the bend is the one with the least value of AARE.

4.3. Performance Analysis before Vertical 90° Bend

Results of model performance before the bend are presented in this section.

4.3.1 Performance of MLP models for the prediction of average void fraction before bend

Result of Table 4 shows that both MLP algorithms developed for the prediction of average void fraction before the vertical 90o bend were good as seen from the small values of AARE and the closeness of R to unity in both cases. However, the model based on the Levenberg-Marquardt algorithm is preferred since it has the smallest value of AARE. The Results for training and validation also showed that both MLP models performed satisfactorily, but only result of test data was used as bases for assessing model performance. Figures 6a and 6b show the variation of MSE with number of iterations for the two MLP models (Gradient descent and Levenberg-Marquardt algorithm) developed for the prediction of average void fraction before the bend. The plots show a decrease in the MSE with number of iteration, which is an indication of error convergence. Iteration is stopped after 10000 and 100 iterations respectively as there is no significant improvement after these points.

It is important to note that besides closeness of model results to experimental data, the MSE curve for both validation and testing must follow similar pattern for the models to be reliable over the entire range of data

set (Bar & Das 2012). This is to eliminate the problem associated with poor data distribution and/or partitioning for training, validation and testing. It is also important to note that validation and testing data do not participate in the weight update process, though validation data is used to stop training when necessary to avoid over-fitting. The performance plots of Figures 6a and 6b show similar trends for validation and testing, thus the models show good generalisation property and can be relied upon over the entire range of data set.

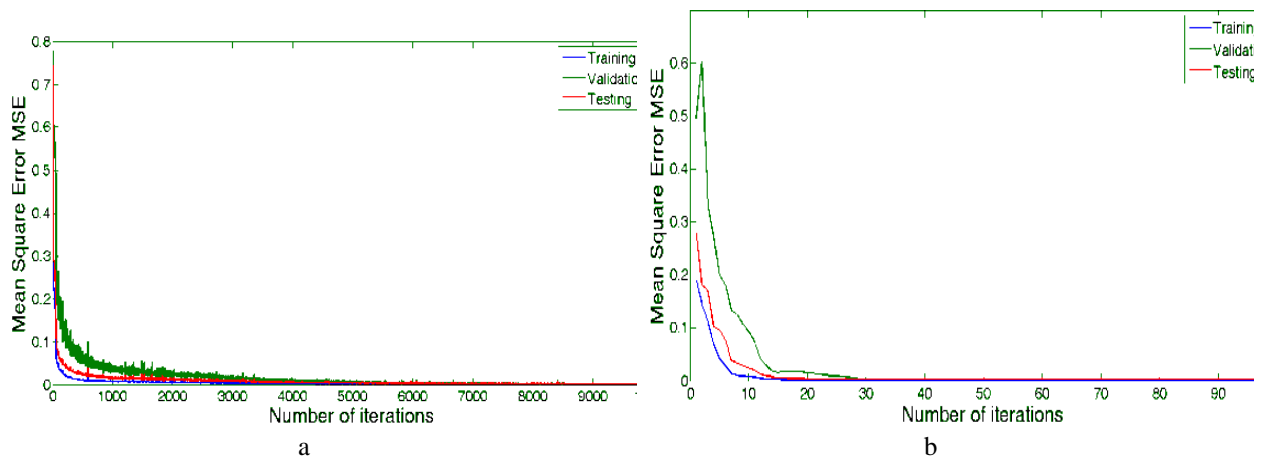
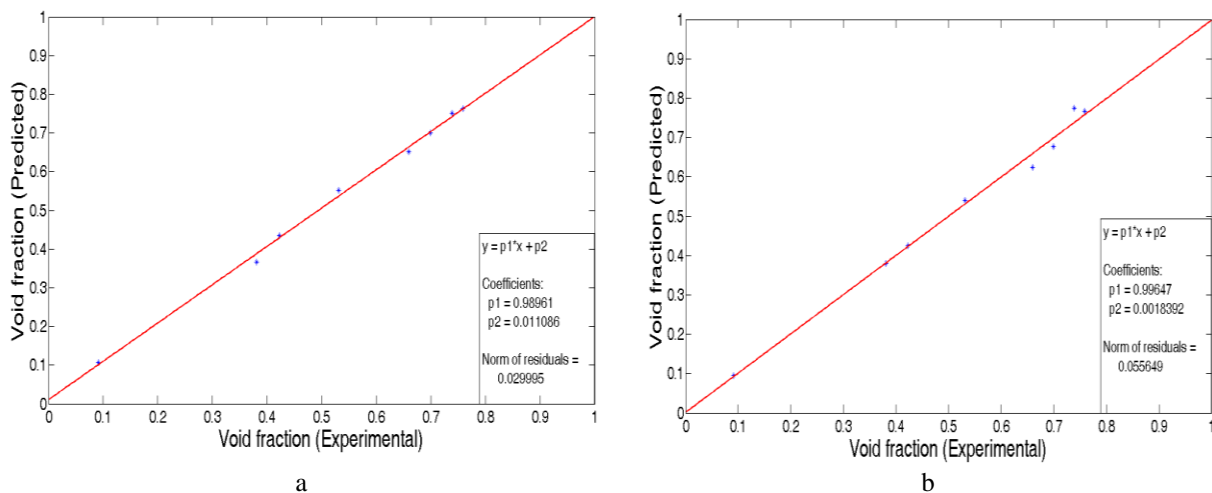


Fig. 6. Variation of MSE with number of iterations for prediction of average void fraction before bend: (a) GDMV model (b) LM model

Figures 7a and 7b are regression plots of test data for the two MLP models developed for the prediction of average void fraction before the vertical 90° bend. The plots are linear with most of the points close to or directly on the line. Also the intercept of the line is close to zero and slope close to one, thus given an almost perfect correlation between experimental and predicted values of average void fraction before bend. These plots further justify the reliability of the proposed models.



Figures 7 (a) and (b). Regression plot of test data before 90° bend for prediction of average void fraction: (a) GDMV model (b) LM model

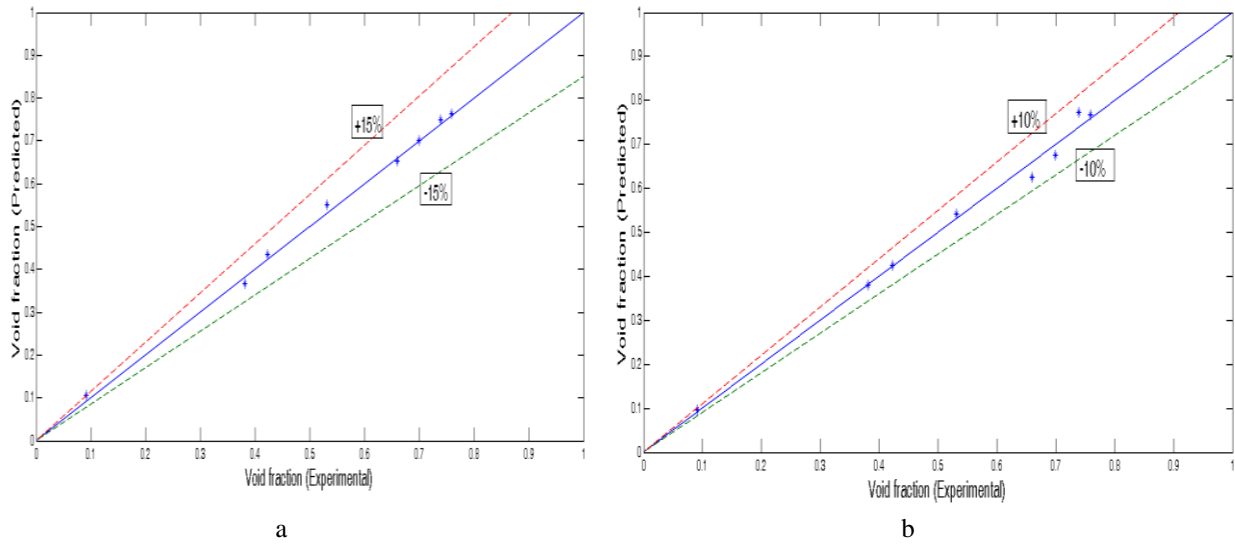


Figure 7 (c) and (d) Comparison between predicted and experimental void fraction for test data before 90°: (c) GDMV model (d) LM model

Results of Figure 7 c and & d show that all the test data predicted by the GDMV model and LM model were with $\pm 15\%$ and $\pm 10\%$ of the experimental data respectively. This further confirms that the LM model performed better for the prediction of average void fraction before the bend.

Table 5 gives a comparison between experimental and predicted average void fraction before the bend. The results showed that predictions for both models were close to experimental results especially at low liquid superficial velocities.

Table 5. Comparison between experimental and predicted average void fraction of air/silicone oil two-phase flow before vertical 90° bend

U_{SL}	U_{SG}	Experimental average void fraction	GDMV model predicted average void fraction	LM model predicted average void fraction
0.050	0.344	0.3806	0.3668	0.3789
0.050	1.418	0.6592	0.6522	0.6249
0.050	1.891	0.6990	0.7008	0.6759
0.050	2.836	0.7591	0.7628	0.7665
0.140	0.047	0.0910	0.1067	0.0954
0.140	0.544	0.4225	0.4352	0.4250
0.140	0.945	0.5315	0.5513	0.5409
0.140	2.836	0.7389	0.7503	0.7739

4.3.2. Performance of MLP models for the prediction of PDF of void fraction before bend

Both MLP models developed for the prediction of PDF of void fraction after the bend also performed excellently. However, the model based on Levenberg-Marquardt algorithm is preferred since it has a smaller value of AARE. MSE plot (Figures 8a and 8b) also show a consistent pattern for training, validation and testing.

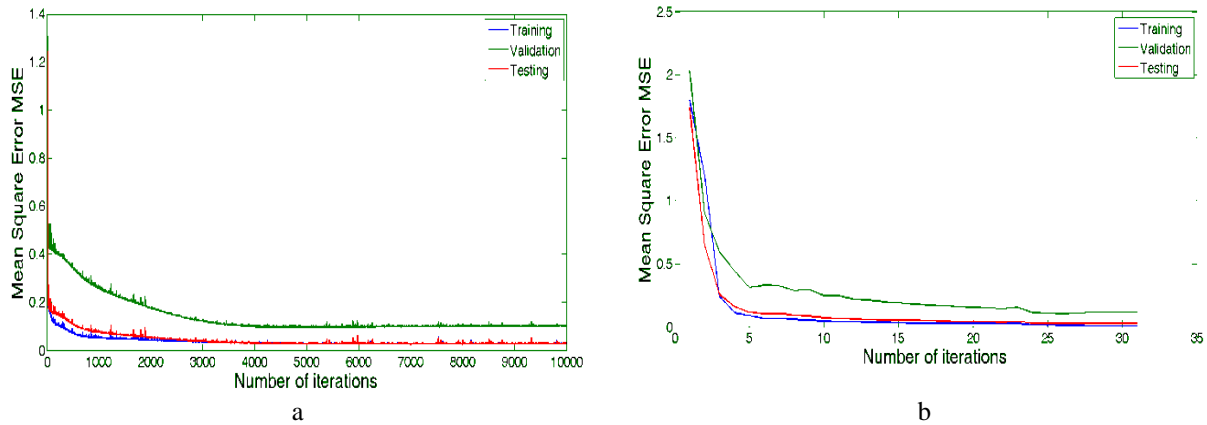


Fig. 8. Variation of MSE with number of iterations for prediction of PDF of void fraction before the bend. (a) GDMV model (b) LM model

Regression plot for test data is shown in Figures 9a and 9b. These plots further validate the MLP models.

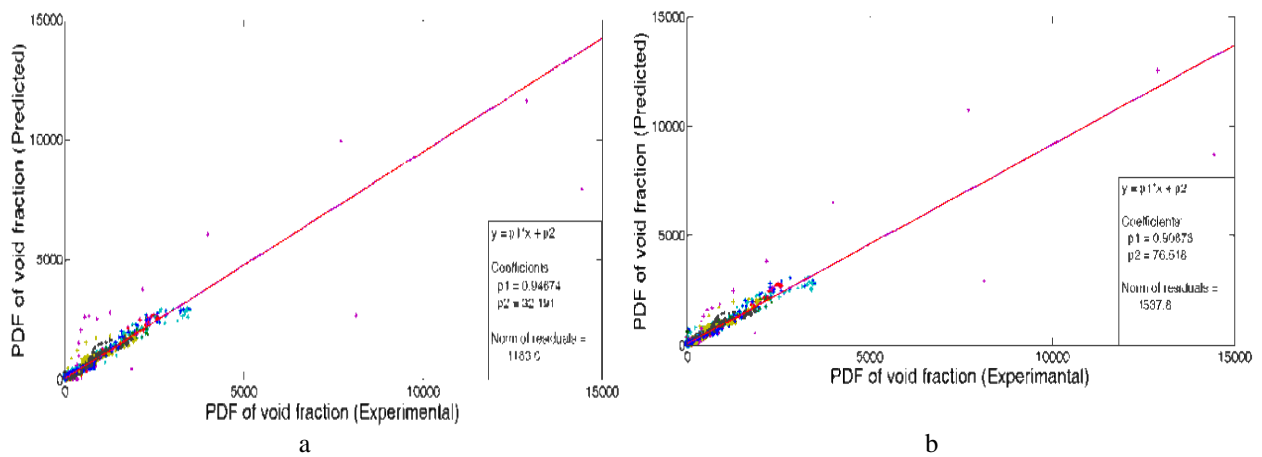
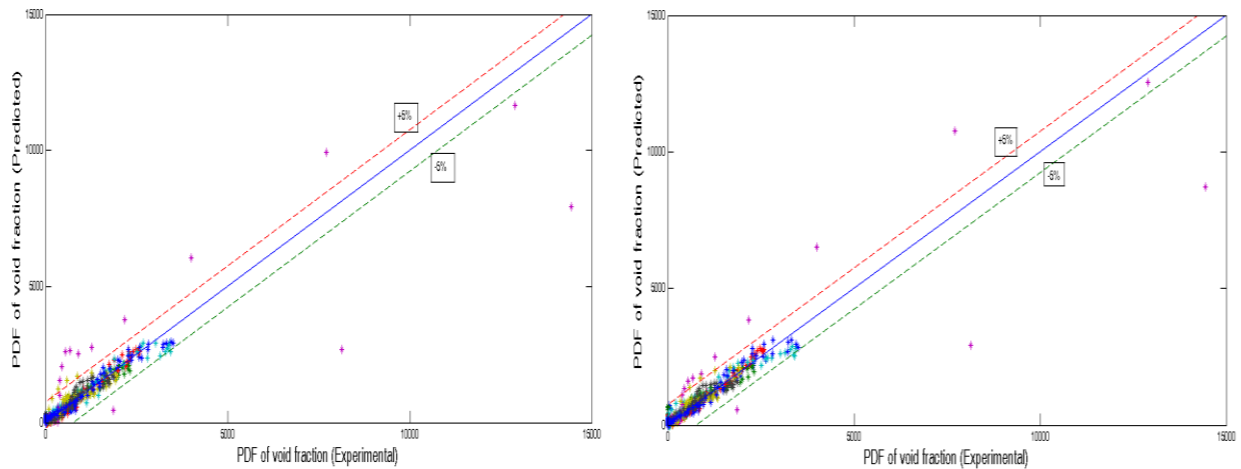


Figure 9 (a) and (b). Regression plot of test data before 90° bend for prediction of PDF of void fraction: (a) GDMV model (b) LM model



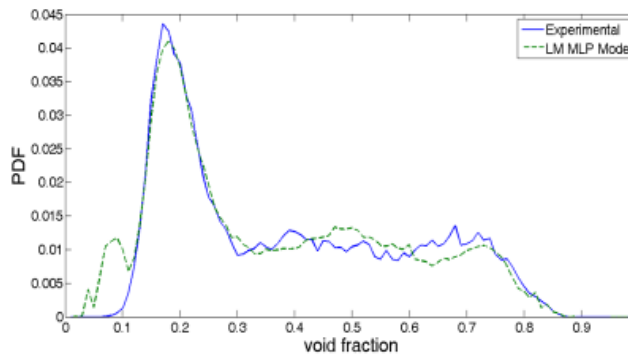
a

b

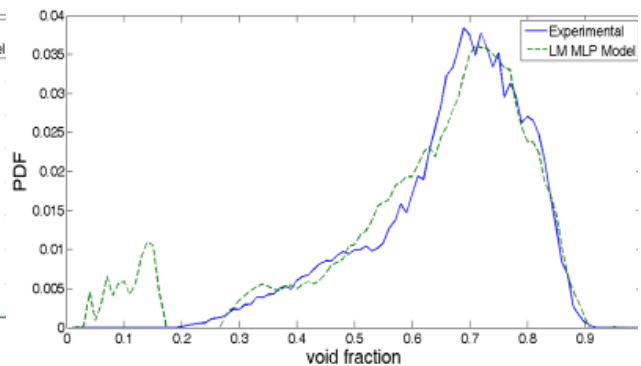
Figure 9 (c) and (d). Comparison between Predicted and Experimental PDF of void fraction before bend. (a) GDMV model (b) LM model

Figures 9c and 9d show that both MLP models developed for the prediction of PDF of void fraction before the bend predicted over 90% of the data with $\pm 5\%$ of the experimental values with the model based on Levenberg-Marquardt algorithm again giving slightly better predictions.

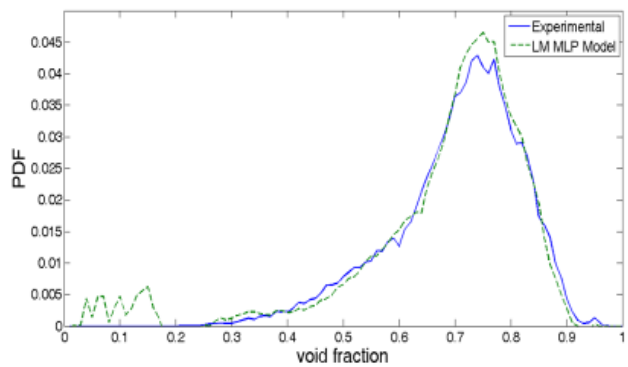
Figures 10a to 10h show comparisons (at various values of U_{SG} and U_{SL}) of the predicted PDF of void fraction before the bend with those from experimental data for MLP model based on the Levenberg-Marquardt algorithm. The results depicted show that the MLP model predicts the PDF of void fraction before the vertical 90° bend to a reasonable level of accuracy over a wide range of data set.



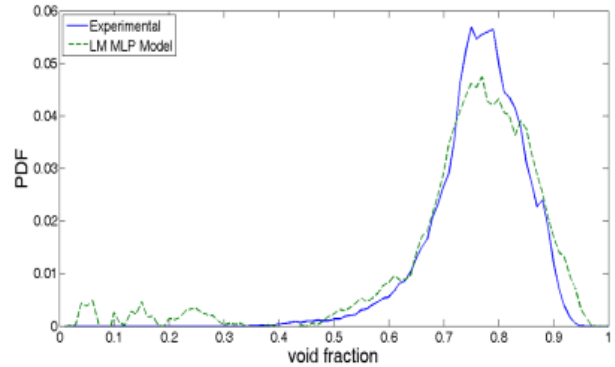
(a) $U_{SL}=0.05$ m/s $U_{SG}=0.344$ m/s



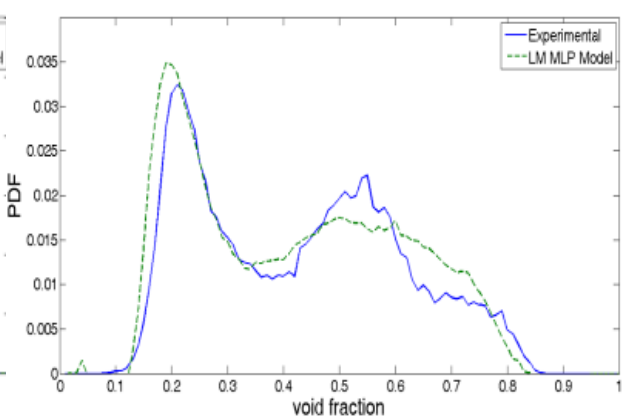
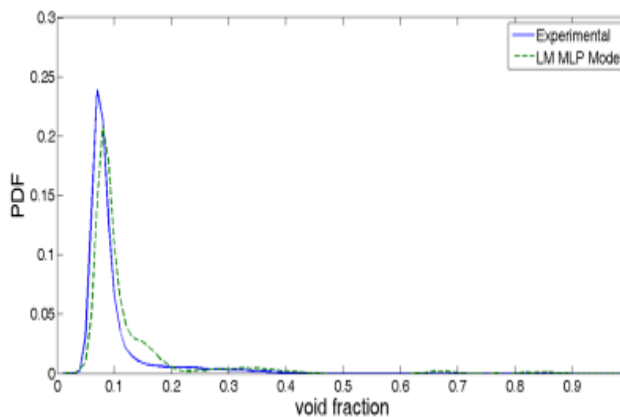
(b) $U_{SL}=0.05$ m/s $U_{SG}=1.418$ m/s



(c) $U_{SL}=0.05$ m/s $U_{SG}=1.891$ m/s



(d) $U_{SL}=0.05$ m/s $U_{SG}=2.836$ m/s



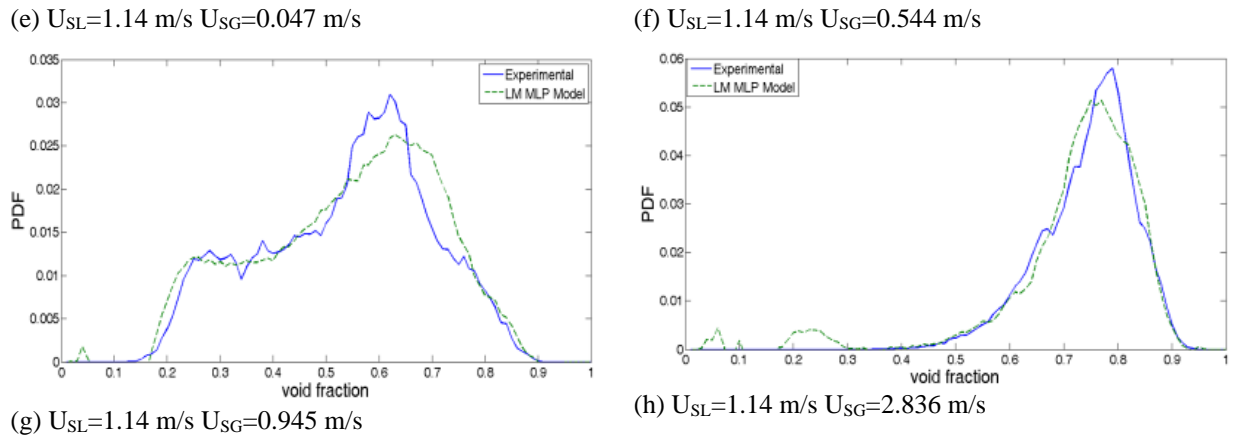


Fig. 10. (LM model): Comparison between Predicted and Experimental PDF of void fraction before bend

Careful inspections of Figures 10a-h reveal that models predictions were particularly good in Figures 10a, 10, 10c, 10d, 10g and 10h. The results of Figures 10a, 10b, 10c, 10d, 10g and 10h show that the model can be used to classify flow pattern before the bend with great confidence.

4.4. Performance Analysis Immediately after Vertical 90° Bend

4.4.1 Performance of MLP models for the prediction of average void fraction after bend

A first look at the results of Table 4 for test data set gives an indication of excellent model performance for both MLP algorithms developed for the prediction of average void fraction immediately after the vertical 90° bend as can be seen from the small values of AARE and the closeness of R to unity in both cases. However results from validation data set show that the values of R for both models were not close to unity. For an MLP model to be valid, both validation and testing performance curve must follow similar pattern. Figures 11a and 11b give the variation of MSE with number of iterations for the two MLP models developed for the prediction of average void fraction immediately after the bend. Figure 11a show a significant divergence in the patterns traced by the validation MSE and the testing MSE. The implication of this would be poor generalisation capability of the model. This significant divergence could be attributed to two things, first; the flow immediately after the bend is not fully developed and second; poor data distribution and/or partitioning among training, validation and testing. Similar conclusion can be drawn from Figure 11b. Even though the divergence between the MSE plots for validation and testing is not well pronounced in this case there is still a significant difference in their patterns.

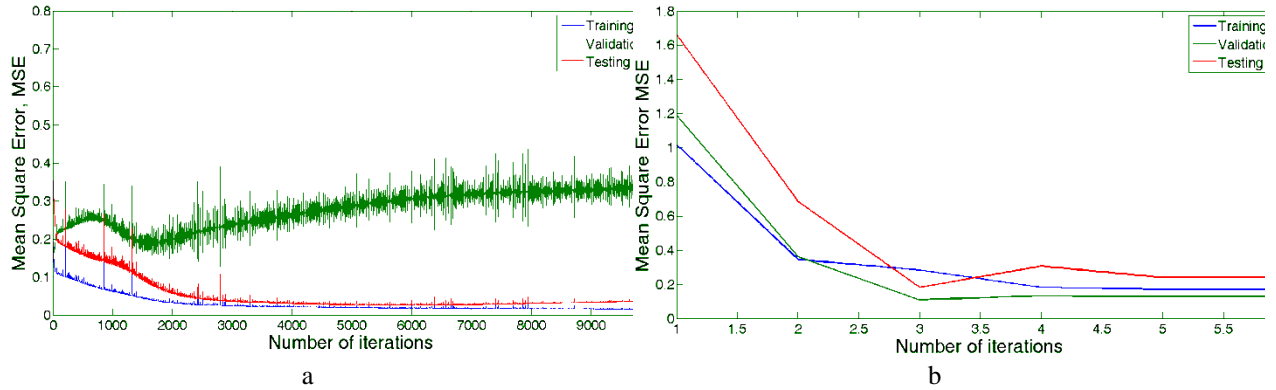


Fig. 11. Variation of MSE with number of iterations for prediction of average void fraction after bend: (a) GDMV model (b) LM model

Figures 12a and 12b are regression plots of test data for the two MLP models developed for the prediction of average void fraction immediately after the vertical 90° bend. These plots again suggest that the models give a good representation of the data. However Figures 13a and 13b, which represents the regression plots for the validation data sets, indicates that the models can only be useful for a limited range of data set.

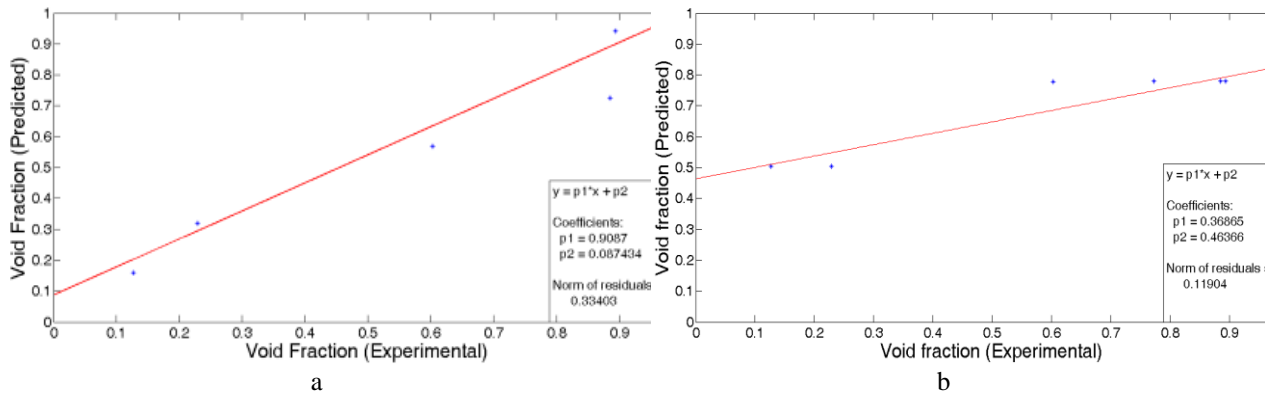


Fig. 12. Regression plot of test data after 90° bend for prediction of average void fraction: (a) GDMV model (b) LM model

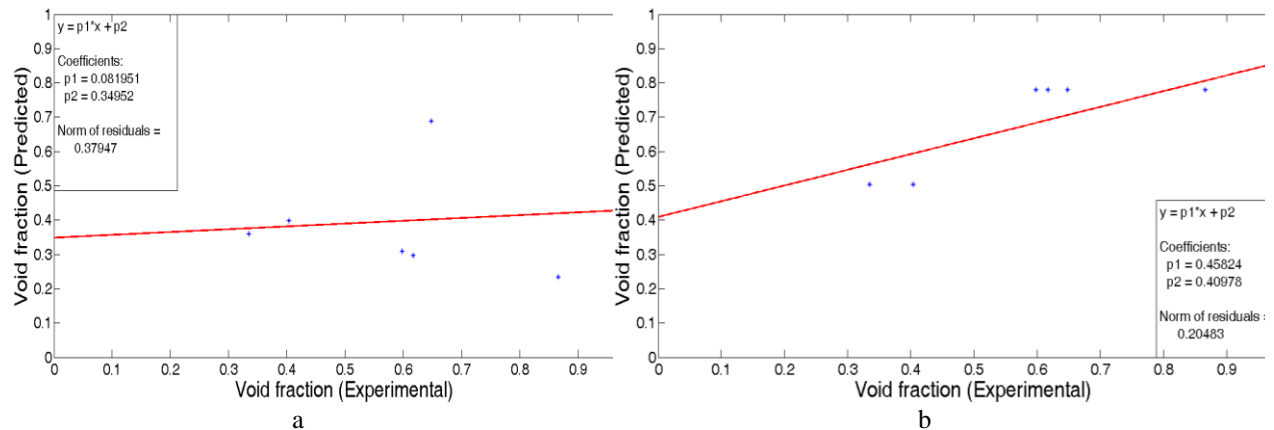


Fig. 13. Regression plot of validation data after 90° bend for prediction of average void fraction: (a) GDMV model (b) LM model

The model based on the gradient descent with momentum term and variable steps size gives a better performance when comparing the two MLP models based on their AARE.

Table 6: Comparison between experimental and predicted average void fraction of air/silicone oil two-phase flow after vertical 90° bend

U_{SL}	U_{SG}	Experimental average void fraction	GDMV model predicted average void fraction	LM model predicted average void fraction
0.050	1.418	0.9941	0.9344	0.7807
0.050	1.891	0.8941	0.9415	0.7807
0.050	2.836	0.8857	0.7256	0.7807
0.140	0.047	0.1274	0.1599	0.5033
0.140	0.544	0.6032	0.5680	0.7776
0.140	1.891	0.7728	1.0578	0.7807
0.380	0.061	0.2289	0.3196	0.5033

4.4.2. Performance of MLP models for the prediction of PDF of void fraction after bend

Results of Table 4 shows that both MLP algorithms developed for the prediction of PDF of void fraction after the vertical 90° bend does not give a good representation of the testing and validation data sets. This is seen from fairly large values of AARE and the lack of closeness of R to unity in both cases. However, the model based on gradient descent algorithm is preferred since it has a smaller value of AARE. Figures 14a and 14b give the variation of MSE with number of iterations for the two MLP models developed for the prediction of PDF of void fraction after the bend. The plots show a divergence in the performance function for validation and testing. This further highlights the lack of generality of the models.

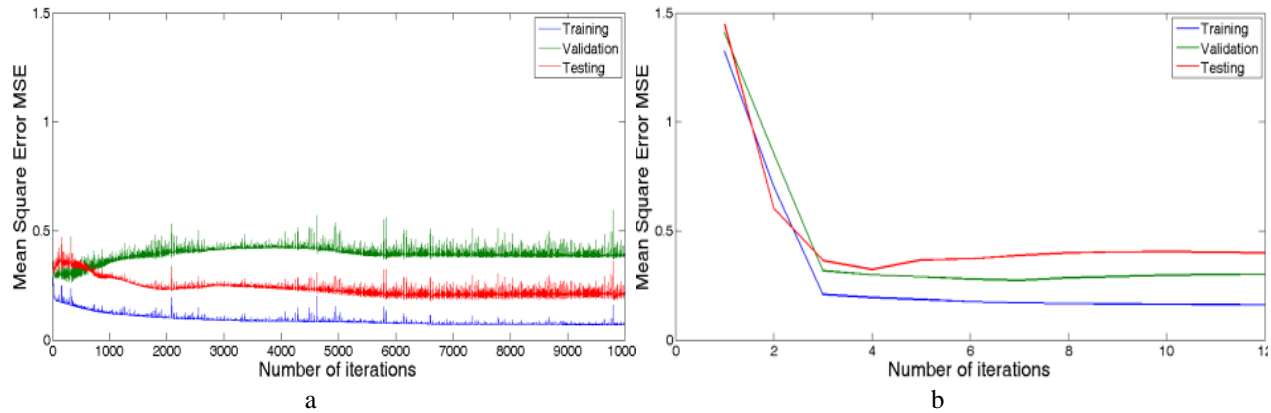


Fig. 14. Variation of MSE with number of iterations for prediction of PDF of void fraction after the bend: (a) GDMV model (b) LM model

Figures 15a and 15b are regression plots for test data for the two MLP models developed for the prediction of PDF of void fraction immediately after the vertical 90° bend. Careful inspection show that the intercept of both curves are close to the origin, however a number of data points do not fall close to the line of best fit. The results further indicate the lack of reliability of the models in predicting the PDF of void fraction immediately after the vertical 90° bend.

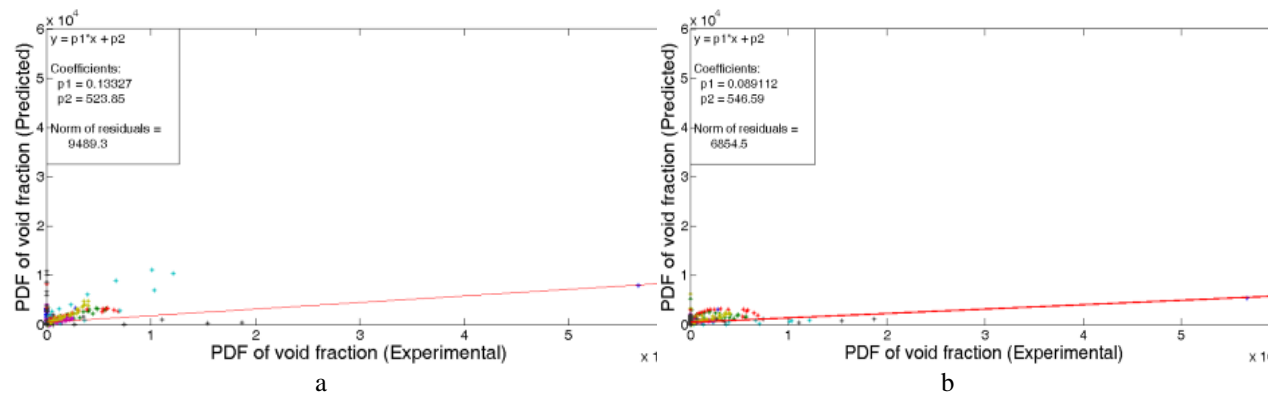


Fig. 15. Regression plot of test data after 90° bend of gradient descent with momentum term and variable step size model for prediction of PDF of void fraction: (a) GDMV model (b) LM model

Figures 16a to 16g give comparisons between predicted and experimental PDF of void fraction (at various values of U_{SG} and U_{SL}) for MLP model based on gradient descent algorithm. The results depicted show that the developed model predicts the PDF of void fraction for gas-liquid flow after vertical 90° bends only within limited range of data sets.

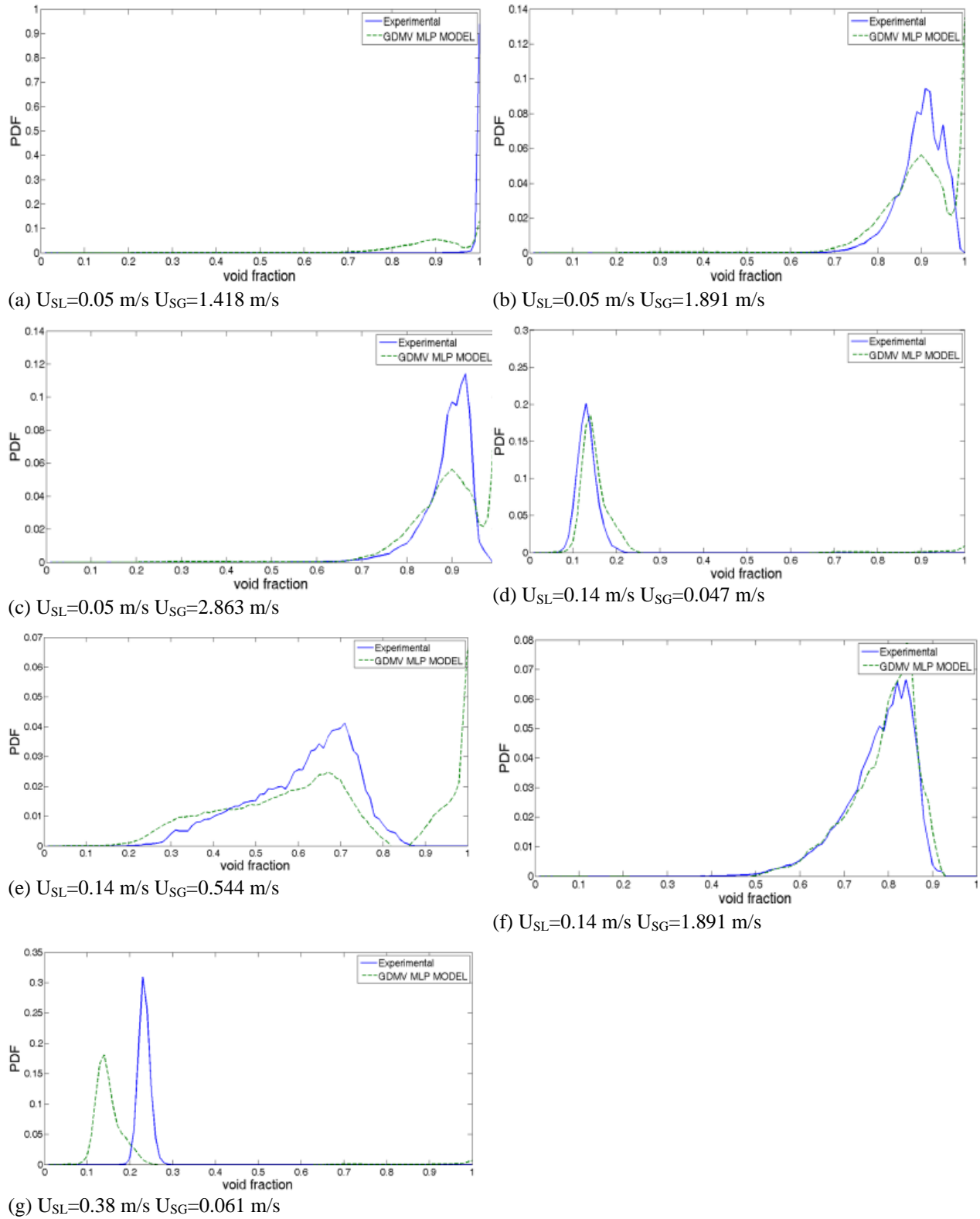


Fig. 16. (GDMV model): Comparison between Predicted and Experimental PDF of void fraction after bend

Careful inspections of Figures 16a-g show that the model prediction as depicted in Figures 16d, 16e and 16f are good while model predictions as depicted in Figures 16a, 16b, 16c and 16g are not very good. These results indicate that the model can only be used to predict flow behaviour after the bend over a limited range of data.

The lack of generality of the MLP models could be associated to two things; one is the fact that the flow is not fully developed and the other is poor data distribution/partitioning among training, validation and testing. The latter is taken care by data redistribution and the use of different partitioning ratio. The data was redistributed using interleaved indices in as opposed to random indices and the data partitioning ratio changed from 6:2:2 to 4:1:1. Similar results were obtained and the models still showed poor generalisation properties.

4.5. Results of Data Interpolation/Extrapolation before 90° Bends

The following liquid superficial velocities were used to test the best performing models at various gas superficial velocities.

$$U_{SL}=0.02\text{ms}^{-1}, U_{SL}=0.15\text{ms}^{-1}, U_{SL}=0.30\text{ms}^{-1}, U_{SL}=0.45\text{ms}^{-1}.$$

Figure 17 gives a plot of predicted average void fraction against gas superficial velocity at liquid superficial velocities not covered by experiment. The plot patterns are in close conformity with expected patterns especially at small and large gas superficial velocities. At intermediate gas superficial velocities the model predictions are not very accurate as can be seen in the crossing of lines.

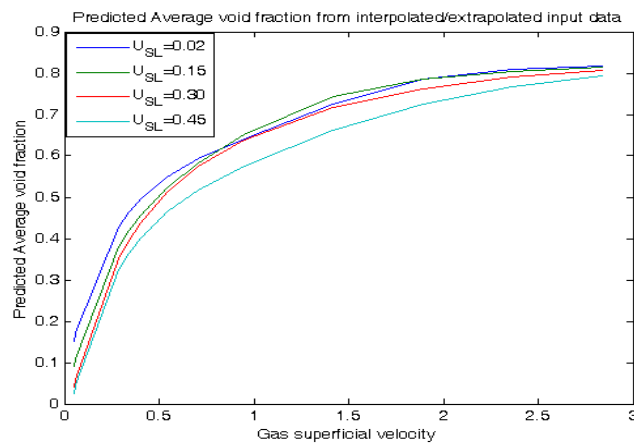


Fig. 17. Plot of predicted average void fraction before bend against gas superficial velocities for various liquid superficial velocities different from those covered by experiment.

Figures 18a to 18d are plots of predicted PDF of void fraction before bend against gas superficial velocities for various liquid superficial velocities different from those covered by experiment.

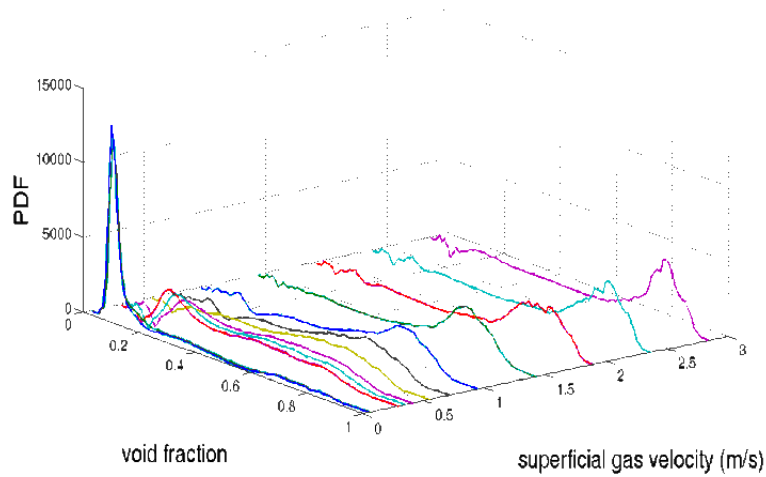


Fig. 18a. Plot of predicted PDF of void fraction before bend against gas superficial velocities for various liquid superficial velocities different from those covered by experiment ($U_{SL} = 0.02 \text{ ms}^{-1}$)

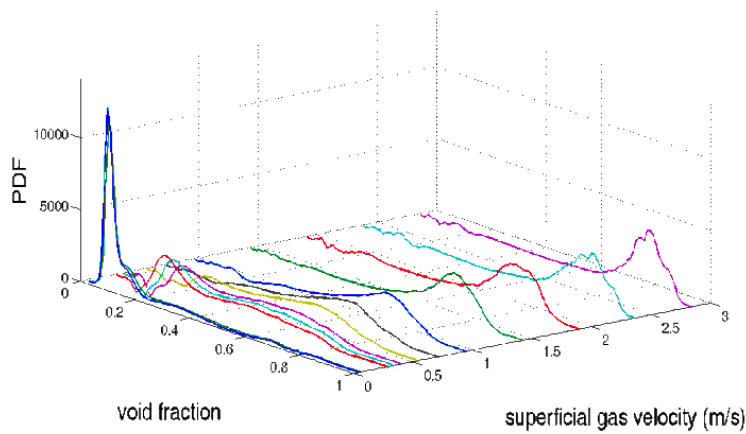


Fig. 18b: Plot of predicted PDF of void fraction before bend against gas superficial velocities for various liquid superficial velocities different from those covered by experiment ($U_{SL} = 0.15 \text{ ms}^{-1}$)

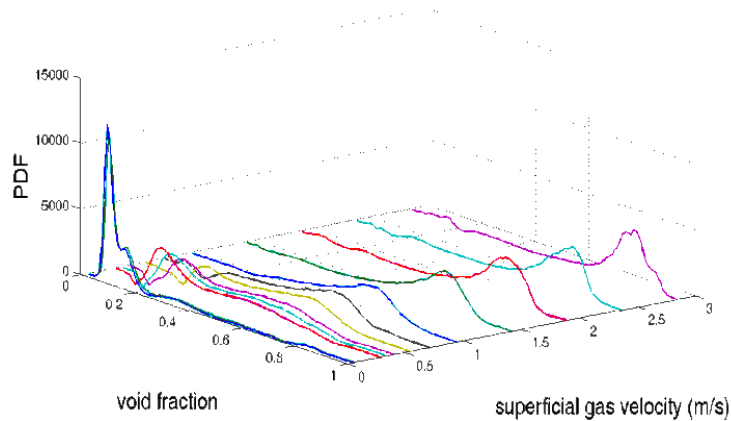


Fig. 18c: Plot of predicted PDF of void fraction before bend against gas superficial velocities for various liquid superficial velocities different from those covered by experiment ($U_{SL} = 0.30 \text{ ms}^{-1}$)

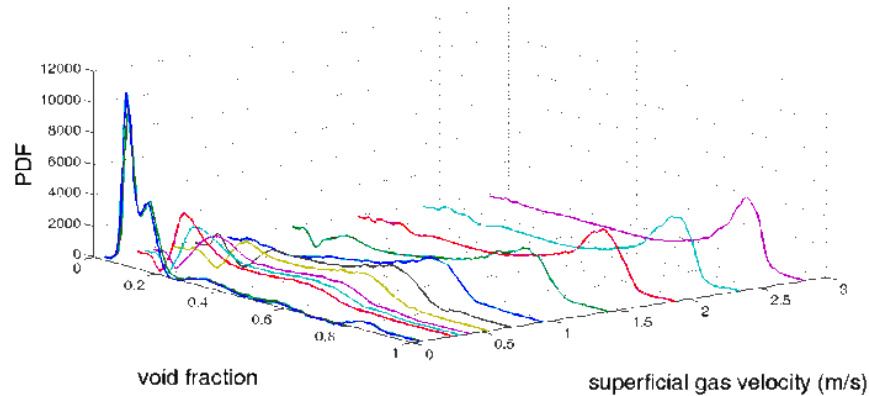


Fig. 18d: Plot of predicted PDF of void fraction before bend against gas superficial velocities for various liquid superficial velocities different from those covered by experiment ($U_{SL} = 0.45 \text{ ms}^{-1}$)

Plot patterns of Figures 18a to 18d follow expected patterns of PDF of void fraction as gas and liquid superficial velocities changes. This patterns show the changes in flow characteristics from bubbly flow to churn flow as gas superficial velocities increases.

5. Conclusions

In this work, Multilayer Perceptron Modelling (MLP) models have been developed to predict two-phase average void fraction and PDF of void fraction in 90° bends. The experiment data were from experiments performed in earlier work in a flow domain of 6 m long vertical pipe with a 67 mm internal diameter connected to a 2 m long flow-line via a vertical 90° bend (bend radius of 154 mm) at various liquid and gas superficial velocities.

Model optimization was carried out by varying network configuration while monitoring the generalisation error (cross validation error). The developed models were trained using feed-forward approach. A comparison of the results obtained from model predictions and experiments both before and after the vertical 90° bend has been successfully carried.

The models developed for the prediction of average void fraction and PDF of void fraction before the bend performed very well. However, the AARE confirmed that the best model for prediction of average void fraction before bend is the MLP model trained with Levenberg-Marquardt algorithm in the hidden and output layer with, having three (3) neurons in the hidden layer. The values of AARE and R for this MLP model are 0.0274 and 0.9958 respectively. The AARE also confirmed that the best model for prediction of PDF of void fraction before the bend is the MLP model trained with Levenberg-Marquardt algorithm in the hidden and output layer, having eleven (11) neurons in the hidden layer. The values of AARE and R for this MLP model are 0.7866 and 0.9342 respectively.

The models proposed for the prediction of average void fraction and PDF of void fraction after the bend showed weak generalisation properties. However, the MLP model based on gradient descent algorithm gave better performance for predicting average void fraction after the bend, with AARE and R values of 0.1961 and 0.9156 respectively. Also, the MLP model based on gradient descent algorithm having four (4) neurons in the hidden layer performed best for the prediction of PDF of void fraction after the bend. The values of AARE and R for this MLP model are 1.5740 and 0.4507 respectively.

The results show that MLP models are effective in predicting average void fraction and PDF of void fraction before the bend but are not effective for predicting after the bend scenario because the flow is not fully developed. Similarly the modified empirical model showed good results for prediction before the bend but could not predict average void fraction after the bend.

References

- Abdulkadir, M., 2011. Experimental and Computational Fluid Dynamics (CFD) Studies of Gas-Liquid Flow in Bends. The University of Nottingham.
- Abdulkadir, M. et al., 2013. Experimental study of hydrodynamic behaviour of slug flow in a vertical riser. *Chemical Engineering Science*, 106, pp.60–15.
- Abdulkadir, M. et al., 2011. Interrogating the effect of 90o bends on air-silicone oil flows using advanced instrumentation. *Chemical Engineering Science*, 66(11), pp.2453–2467. Available at: <http://dx.doi.org/10.1016/j.ces.2011.03.006>.
- Asghar, A., Masoud, R. & Abdulaziz, A., 2009. CFD and artificial neural network modeling of two-phase flow pressure drop. *International Communications in Heat and Mass transfer*, 8(36), pp.850–856.
- Ayoub, M.A. & Demiral, B.M., 2011. Application of Resilient Back-Propagation Neural Networks for Generating a Universal Pressure Drop Model in Pipelines. *UNIVERSITY of KHARTOUM ENGINEERING JOURNAL*, 1(2), pp.9–21.
- Bansal, A.R., Kanuffman, J. & Weitz, R.R., 1993. Comparing the modelling performance of regression and neural networks as data quality varies: A Business value approach. *Journal of Management Information Systems*, 10, pp.11 – 32.
- Bar, N. & Das, S.K., 2012. Gas-non-Newtonian Liquid Flow Through Horizontal Pipe – Gas Holdup and Pressure Drop Prediction using Multilayer Perceptron. *American Journal of Fluid Dynamics*, 2(3), pp.7–16.
- Bar, N., Das, S.K. & Biswas, M.N., 2013. Prediction of Frictional Pressure Drop Using Artificial Neural Network for Air-water Flow through U-bends. *Procedia Technology*, 10, pp.813–821. Available at: <http://www.sciencedirect.com/science/article/pii/S2212017313005884>.
- Barnard, E. & Wessels, L., 1992. Extrapolation and interpolation in Neural Network Classifiers. *IEEE Control Systems*, 12, pp.50–53.
- Carlos, G., 2011. Artificial neural networks for beginners.
- Carver, M.B., 1984. Numerical computation of phase separation in two fluid flow. *ASME Paper*, 6, p.153.

- Carver, M.B. & Salcudean, M., 1986. Three-dimensional numerical modelling of phase distribution of two- fluid flow in elbows and return bends. *Numerical Heat Transfer*, 10, pp.229–251.
- Ellul, I.R. & Issa, R.I., 1987. Prediction of the flow of interspersed gas and liquid phases through pipe bends. *Transaction of Institution of Chemical Engineers*, 65, pp.84–96.
- Gardner, G.C. & Neller, P.H., 1969. Phase distributions flow of an air-water mixture round bends and past obstructions. In *Proceedings of Institution of Mechanical Engineers*. pp. 93–101.
- Hao, Y. & Wilamowski, B.M., 2010. Levenberg–Marquardt Training. In *Industrial Electronics Handbook: INTELLIGENT SYSTEMS*. Auburn: Auburn University, pp. 1–16.
- Hernandez, L. et al., 2006. Fast classification of two-phase flow regimes based on conductivity signals and artificial neural networks. *Measurement Science and Technology*, 17.
- Karimi, H. et al., 2014. Prediction of flow pattern in vertical gas-liquid flow using pressure fluctuations and artificial neural network. In *The 8th International Chemical Engineering Congress and Exhibition (IChEC 2014)*. Kish, Iran.
- Legius, H.J., Narumo, T.J. & Van-den-Akker, H.E.A., 1995. Measurements on wave propagation and bubble and slug velocities in concurrent upward two-phase flow. In: Celuta, G. P., and Shah, R. K. (Eds), *Two-Phase Flow Modelling and Experimentation*, Rome, pp.907–914.
- Mark, H.B., Martin, T.H. & Howard, B.D., 2012. *Neural Network Toolbox (Matlab User’s Guide, R2012b)*. , pp.20–30.
- Mustafa, A., Moustafa, E. & Abdulsalam, A., 2015. Two phase flow regime identification using Artificial Neural Network with non-linear normalization. , 133.
- Nasseh, S. et al., 2007. Predicting pressure drop in venturi scrubbers with artificial neural networks. *Journal of Hazardous Materials*, 143, pp.144–149.
- Nirjhar, B. & Sudip, K.D., 2013. Prediction of flow regime for air-water flow in circular micro channels using ANN. *Journal of Petroleum Science and Engineering*, 10, pp.813–821.
- Saidj, F. et al., 2014. Experimental investigation of air-water two-phase flow through vertical 90 ° bend. *Experimental Thermal and Fluid Science*, 57, pp.226–234.
- Santoso, B. & Thomas, S.W., 2012. The Identification of Gas-liquid Co-current Two Phase Flow Pattern in a Horizontal Pipe Using the Power Spectral Density and the Artificial Neural Network (ANN). *Modern Applied Science*, 6(9), pp.56–67.
- Soetaert, K. & Herman, P.M.J., 2009. *A practical guide to ecological modelling*. Springer ISBN: 978-1-4020-8623-6.
- Tarun, K.B. & Sudip, K.D., 2007. Non-Newtonian pseudo-plastic liquid flow through small diameter piping components. , 55, pp.156–166.
- Thiele, S. et al., 2008. High-resolution oil-gas two-phase flow measurement with a new capacitance wire-mesh tomography. In *5th International Symposium on Process Tomography*. Poland, Zakopane, pp. 25–26.
- Zhigiang, S. & Z. Hongjian, 2008. Neural networks approach for prediction of gas–liquid two-phase flow pattern based on frequency domain analysis of vortex flow meter signals. *Measurement Science and Technology*, 19, pp.1–8.